Microcomputed tomography colonography for polyp detection in an *in vivo* mouse tumor model

Perry J. Pickhardt*†, Richard B. Halberg†‡, Andrew J. Taylor*, Ben Y. Durkee*, Jason Fine§, Fred T. Lee, Jr.*, and Jamey P. Weichert*¶

Departments of *Radiology and §Biostatistics, University of Wisconsin Medical School, 600 Highland Avenue, Madison, WI 53792; and ‡McArdle Laboratory of Cancer Research, University of Wisconsin, 1400 University Avenue, Madison, WI 53706

Communicated by William F. Dove, University of Wisconsin, Madison, WI, December 31, 2004 (received for review December 28, 2004)

This study was initiated to evaluate the efficacy of negative contrast-enhanced microcomputed tomography (microCT) colonography for the noninvasive detection of colonic tumors in living mice. After colonic preparation, 20 anesthetized congenic mice were scanned with high-resolution microCT. Images were displayed by using commercial visualization software and interpreted by two gastrointestinal radiologists, who were unaware of tumor prevalence and findings at gross pathology. Two-dimensional multiplanar images were assessed by using a five-point scale to distinguish colonic tumors (polyps) from fecal pellets (5 = definitely a tumor, 4 = probably a tumor, 3 = indeterminate, 2 = probably not a tumor, 1 = definitely not a tumor). Gross pathologic evaluation of excised mouse colons served as the reference standard. Data analysis included dichotomizing results, with 1–2 indicating no tumor and 3–5 indicating tumor and also receiver operator characteristic curve analysis with area under the curve for threshold-independent assessment. A total of 41 colonic polyps in 18 of the 20 mice were identified at gross examination on necropsy, of which 30 measured 2–5 mm and 11 measured <2 mm in size. The pooled per-polyp sensitivity for lesions >2 mm was 93.3% (56/60). The pooled per-mouse sensitivity for polyps >2 mm was 97.1% (33/34). Pooled specificity for distinguishing fecal pellets from tumor was 98.5% (65/66). The combined area under the curve from receiver operator characteristic curve analysis was 0.810 ± 0.038 (95% confidence interval, 0.730–0.890). These findings indicate that accurate noninvasive longitudinal monitoring of colon tumor progression or response to various therapies is now technically feasible in live mice by using this microCT colonography method.

colonic neoplasm

Colorectal cancer remains the second leading cause of cancer-related human mortality in the United States, despite the fact that the great majority of these malignancies are likely to be preventable through routine screening (1, 2). Computed tomographic (CT) colonography, also known as virtual colonoscopy, is a rapidly evolving x-ray technique that has recently been shown to be an accurate screening tool for the detection of colorectal polyps in humans (3). When state-of-the-art methods are applied, CT colonography has the ability to noninvasively detect significant lesions missed at conventional colonoscopy, the current gold standard (4). The preferred embodiment for CT colonography interpretation includes both 2D and 3D imaging displays for polyp detection, with an emphasis on the latter (5, 6). CT colonography holds significant promise for increasing compliance rates in screening for early colonic lesions. In addition to screening for polyps, CT colonography also can provide a means for noninvasive surveillance of unresected polyps (7). As a preclinical bridge to human trials, CT colonography needs to be applied to existing mouse models of colorectal cancer by using microcomputed tomography (microCT), a recent development that allows for high-resolution, noninvasive CT imaging in small animals (8, 9).

The primary goal of this study was to develop and establish proof of concept that microCT colonography is a feasible and reliable test for *in vivo* detection of colonic polyps in mice that can reliably distinguish tumor from luminal fecal pellets. The potential implications of our findings will be discussed.

Materials and Methods

Mouse Tumor Model. All animal studies were conducted under approved guidelines set forth by the Institutional Animal Care and Use Committee of the American Association for Assessment and Accreditation of Laboratory Animal Care at the University of Wisconsin. The congenic strain used for this study was created by introducing the *Min* allele of the *Apc* gene (10) from the C57BL/6J genetic background onto the C57BL/6J $Tyr^{c\text{-}2J}/+$ genetic background by backcrossing for 10 generations. This congenic strain developed an average of 2.1 ± 0.4 (SEM) colonic tumors (range, 0–7) in 20 mice. This strain represents a good candidate for evaluation of microCT colonography because the number of colonic tumors is relatively high, compared with other mouse models of human colorectal cancer (10).

Mouse Bowel Preparation. A total of 20 congenic mice were selected for microCT scanning. The mice were provided a diet of fresh vegetables, raw unsalted sunflower nuts, and water for 2 days ad libitum, followed by cherry-flavored NuLYTELY (Braintree Scientific) for 16 h before microCT scanning. In our experience, this dietary approach significantly decreases the streak artifacts in microCT created by bone meal and other high-density fillers that are often found in normal pelleted mouse chow. The 20 mice (17–22 g body weight) were anesthetized with pentobarbital (0.06 mg/g body weight, i.p. injection), given an enema consisting of ≈1–1.5 ml of corn oil, and scanned for colonic tumors by microCT.

MicroCT Scanning. Anesthetized mice were scanned in the prone position immediately after rectal administration of contrast material. Images were acquired on a microCT scanner (MicroCAT I, ImTek, Knoxville, TN) by using the following imaging parameters: 43-kV peaks, 410 μA, 390 steps, 20-min scan duration. No i.v. contrast was administered, nor was an attempt made to gate image acquisition for peristaltic or respiratory motion, given the long acquisition times involved. Image data were reconstructed as 256 × 256 × 256 voxels (200-μm spatial resolution) by using a Shepp-Logan filter with back projection and no beam-hardening correction over an appropriate subvolume. Although much higher resolution is possible with these scanners, it is our experience that these acquisition and reconstruction parameters easily afford more than adequate spatial resolution while minimizing the radiation dose to the live mice.

Abbreviations: AUC, area under the curve; CT, computed tomography; microCT, microcomputed tomography; ROC, receiver operator characteristic.

†P.J.P. and R.B.H. contributed equally to this work.

¶To whom correspondence should be addressed. E-mail: j.weichert@hosp.wisc.edu.

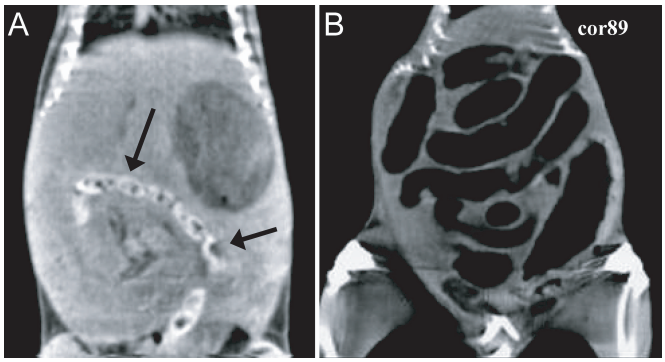

Fig. 1. Ungated coronal microCT images of normal chow-fed (*A*) and low-density, bowel-prepped (*B*) mice. Although fecal pellets (*A*, arrows) are distinguishable by virtue of their relatively high density, the lumen of the intestinal tract is much easier to map after low-density bowel preparation (*B*).

Anesthetized mice were euthanized immediately after CT scanning.

MicroCT Image Interpretation. The microCT image data from each mouse were analyzed by using commercially available visualization software (AMIRA, Version 3.1, TGS, San Diego), which displayed the data as 2D axial, sagittal, and coronal cross-sectional images (Figs. 1 and 2). The lumen of the colon near the rectum was marked by the end of the syringe, which prevented the contrast agent from flowing out during the scan. The radiologists were able to follow the colonic lumen from the rectum to the cecum. Window-level settings for the 2D displays were optimized for polyp detection, similar to that used for CT colonography in humans. Soft-copy interpretation was performed by two experienced gastrointestinal radiologists (P.J.P. and A.J.T.), each of whom was unaware of the findings or tumor prevalence at gross pathology. The readers evaluated the studies for focal colonic findings by using a five-point scale for distinguishing colonic tumors (polyps) from luminal fecal pellets (5 = definitely a tumor, 4 = probably a tumor, 3 = indeterminate/possibly a tumor, 2 = probably not a tumor, 1 = definitely not a tumor). A definite tumor was a mass projecting from the colonic wall composed of homogeneous soft tissue with uniform low density. By contrast, assessments designated as "definitely not a tumor" were heterogeneous collections of low- and high-density material without clear attachment to the colonic wall. In some instances, a focal finding was not specifically assigned a score; the convention in this case was to assign these a score of 0, indicating an even stronger confidence for nontumor than a score of 1. This results in a raw-score scale of 0–5 for focal colonic findings. For each detected lesion, the readers marked the relative location and size on a schematic map of the mouse colon to facilitate matching the radiologic score with retrospective gross pathologic findings on necropsy.

Reference Standard. Gross pathologic inspection of the excised mouse colon served as the gold standard against which the microCT results were compared. Mice were killed immediately after the microCT scan. The colon was removed, opened longitudinally, digitally photographed, washed with PBS, and photographed again. A total of 41 colonic tumors and 33 fecal pellets were identified. The tumors ranged in size from <1 mm to up to 5 mm. This procedure enabled us to coregister tumors and fecal pellets observed during necropsy to those identified and mapped by radiologists by using *in vivo* images.

Data Analysis. For analysis of sensitivity and specificity for colonic polyp detection, confidence scores were first dichotomized by 0–2 indicating no tumor and 3–5 indicating tumor. Performance characteristics also were derived by using a dichotomy point between confidence scores of 3 and 4. Analysis was performed for both a per-polyp and a per-mouse basis. A per-mouse analysis is similar in concept to the per-patient analysis in human CT colonography trials (3), which is a binary consideration for the presence or absence of polyps at a given size threshold. Differences in reader performance were compared by using Fisher's exact test ($P < 0.05$, indicating a statistically significant difference). Finally, we performed a receiver operator characteristic (ROC) curve analysis for threshold-independent evaluation. We obtained area under the curve (AUC), a measure of test accuracy with values closer to 1 being more accurate, for distinguishing tumors from nontumors by microCT. ROC analysis, which plots the true-positive rate against the false-positive rate for the different cutoff points of a diagnostic test, illustrates the tradeoff between sensitivity and specificity for diagnostic tests. Used in conjunction with each other, ROC and AUC determinations allow for assessment of performance that is independent of specific thresholds for calling tumor vs. no tumor.

Results

Of the 41 colonic tumors identified at gross pathologic examination, 2 lesions measured 5 mm in maximal diameter, 7 measured 4 mm, 11 measured 3 mm, 10 measured 2 mm, and 11 measured <2 mm. For the 30 tumors that measured between 2 and 5 mm, the mean was 3.0 mm. Seventeen mice had at least one colonic polyp that measured between 2 and 5 mm; one mouse had two tumors that were <1 mm. Two of the mice showed no tumors at gross evaluation and served as negative controls for the radiological interpretation *in vivo*.

The ability to detect endoluminal lesions was significantly enhanced in low-density bowel-prepped mice relative to normal chow-fed mice (Fig. 1). Although fecal pellets are visible (Fig. 1*A*) by virtue of their increased density in the unprepped mice, it remains virtually impossible to detect intestinal lesions in these animals. Negative contrast enhancement of the bowel (Fig. 1*B*), however, affords a much higher contrast differential in the lumen, thus enhancing the conspicuity of lesions within the lumen.

Table 1. Sensitivity for tumor detection with microCT colonography

Tumor size	Number	Reader 1 sensitivity*		Reader 2 sensitivity*		Pooled sensitivity*	
		Analysis according to polyp					
≥3 mm	20	95.0% (19/20)	90.0% (18/20)	95.0% (19/20)	85.0% (17/20)	95.0% (38/40)	87.5% (35/40)
≥2 mm	30	90.0% (27/30)	73.3% (22/30)	96.7% (29/30)	86.7% (26/30)	93.3% (56/60)	80.0% (48/60)
<2 mm	11	27.3% (3/11)	27.3% (3/11)	54.5% (6/11)	54.5% (6/11)	40.9% (9/22)	40.9% (9/22)
		Analysis according to mouse					
≥3 mm	14	100% (14/14)	92.9% (13/14)	92.9% (13/14)	92.9% (13/14)	96.4% (27/28)	92.9% (26/28)
≥2 mm	17	100% (17/17)	88.2% (15/17)	94.1% (16/17)	94.1% (16/17)	97.1% (33/34)	91.2% (31/34)

*Sensitivity data reported in the left column for each reader are with confidence scores dichotomized by 0–2 indicating no tumor and 3–5 indicating tumor, whereas data in the right column are dichotomized by 0–3 and 4–5, respectively.

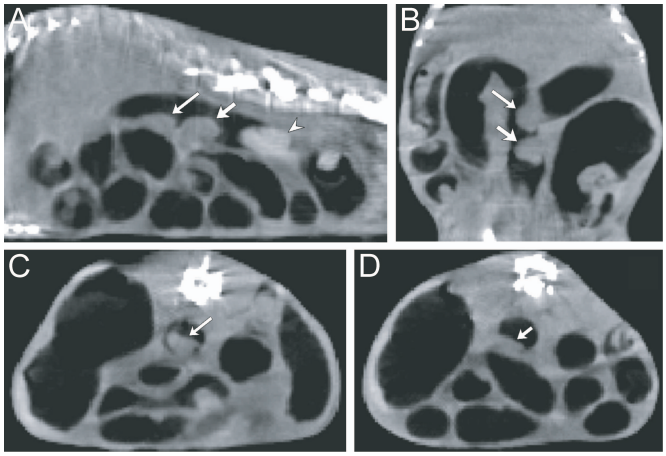

Fig. 2. Ungated, prone, 2D sagittal (*A*), coronal (*B*), and axial (*C* and *D*) images from microCT colonography in an anesthetized mouse show two colonic tumors (arrows) outlined by negative luminal contrast that both measured 2 mm on gross pathologic examination. The lesion that is more cephalad (long arrow) has a flatter morphology, compared with the caudal lesions (short arrow), which have a more sessile polypoid appearance. Both tumors were detected with high confidence by both readers. Note also an adjacent luminal fecal pellet on the sagittal projection (arrowhead), which shows increased density and was recorded as ''definitely not a tumor'' by both readers.

The per-polyp sensitivity for tumor detection with microCT colonography is greatly affected by the size of the colonic tumor as indicated in Table 1. Reliable detection of colonic tumors measuring 2 mm and greater was achieved by both readers (Fig. 2). Pooled sensitivity was >90% for tumors measuring ≥2 mm and 95% for those measuring ≥3 mm (Fig. 3) by using the dichotomy 0–2 indicating no tumor and 3–5 indicating tumor. If confidence scores are dichotomized as 0–3 indicating no tumor and 4–5 indicating tumor, the pooled sensitivity drops to 80% (48/60) at the 2-mm threshold and 88% (35/40) at the 3-mm threshold. Sensitivity was notably decreased for polyps measuring <2 mm. Overall, the differences in performance between the two readers were not statistically significant.

The specificity for distinguishing fecal pellets as nontumor was high, 100% (33/33) for reader 1 and 97% (32/33) for reader 2, and was not affected by whether a confidence score of 3 was considered as tumor or nontumor. In general, fecal pellets are readily distinguished from soft-tissue polyps by microCT because of their increased density and internal heterogeneity. In addition to confirmed tumors and fecal pellets, nine additional sites were scored that lacked definite correlates at gross inspection. Some of these additional sites resulted in false positives, which lower the pooled specificity to 92% (77/84). These false positives probably resulted from ''soft'' fecal material due to treatment with NuLYTELY and would likely be eliminated by flushing the colon with warm PBS before administering contrast agent.

Fig. 3. Digital photograph of an excised mouse colon that has been longitudinally incised shows a single tumor (arrow) that measures ≈3 mm.

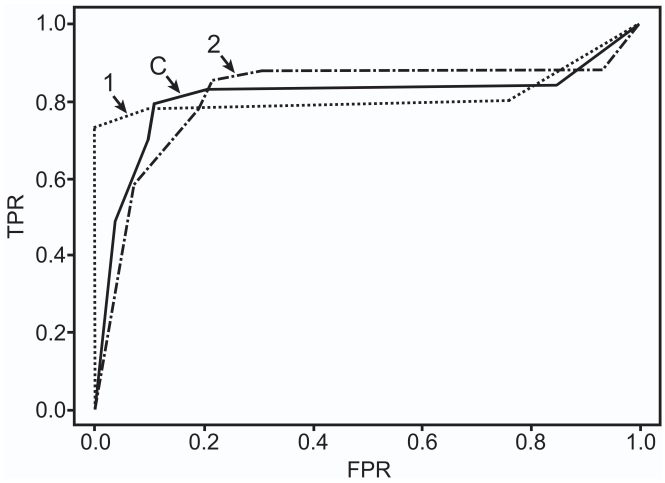

Fig. 4. ROC curves for reader 1, reader 2, and the combination of the two (C) for detecting and distinguishing tumor from nontumor by microCT colonography. The corresponding AUCs are 0.815, 0.815, and 0.810, respectively (see text for more detail). TPR, true positive result; FPR, false positive result.

The resulting ROC curves for reader 1, reader 2, and the combination of the two are presented in Fig. 4, demonstrating clearly the tradeoff between sensitivity and specificity for different possible dichotomies. The AUC (±SE) was 0.815 ± 0.055 for reader 1, 0.815 ± 0.053 for reader 2, and 0.810 ± 0.038 for combined results (95% confidence interval, 0.73–0.89), indicating that this experimental approach accurately identifies colonic tumors in the mouse. The differences in AUC between readers 1 and 2 are very small.

Sensitivity for colorectal polyps with analysis on a per-mouse basis also is shown in Table 1. There were 17 mice with at least one polyp measuring ≥2 mm and 14 mice with at least one polyp measuring ≥3 mm. In general, per-mouse sensitivities were high at both the 2- and 3-mm thresholds, regardless of which dichotomous scoring point is used. Per-mouse specificity for excluding polyps was 100% (3/3) for both readers at the 2-mm threshold, with recorded confidence scores of only 0 and 1 in these cases.

Discussion

Colorectal cancer is the leading cause of cancer deaths among nonsmokers in the United States (1). But unlike other common malignancies that are often fatal, such as lung and breast cancer, the great majority of colorectal cancer deaths are believed to be preventable through early detection and removal of advanced precancerous adenomas (2). In addition, asymptomatic cancers detected by screening have a more favorable prognosis than symptomatic cancers not detected by screening. The primary reason that colorectal cancer remains such a major public health issue is that most adults over age 50 have not been properly screened.

CT colonography, also referred to as CT virtual colonoscopy, represents a promising means by which screening compliance rates could be increased (7). When state-of-the-art 3D techniques are combined with 2D imaging, CT colonography compares favorably and is complementary to conventional colonoscopy for the detection of clinically relevant polyps (3, 4). Beyond asymptomatic screening, CT colonography also holds significant promise for noninvasive surveillance of unresected lesions (7), which includes the potential for monitoring disease progression and response to therapy. An initial evaluation of such noninvasive strategies in small animal models could serve as a direct preclinical bridge to human trials.

In general, the spatial resolution of clinical imaging systems used for human investigation is insufficient for small animal

studies, necessitating the development of dedicated high-resolution systems (8). As a result, imaging systems designed specifically for small-animal research have made significant advances over the past 20 years, including modalities such as MRI, positron-emission tomography, bioluminescence imaging, and CT (8, 9, 11–13). A distinct advantage of noninvasive imaging over more traditional assays is that the experimental animal need not be killed, allowing for longitudinal investigation. In particular, microCT is emerging as a cost-effective and broadly available approach for a number of small animal research applications (8, 9).

X-ray microCT is capable of achieving spatial resolution on the order of 20 μm. To allow for continued study of the animal after imaging, it is important to carefully select appropriate anesthesia, radiation, and contrast media techniques so as not to significantly affect the health of the animal (8, 9). To date, the vast majority of microCT studies have focused on skeletal models because the inherent density of these tissues allows for adequate microCT evaluation without the need for contrast media (14–17). Far fewer nonskeletal microCT studies have been reported and generally involve lung or vascular imaging (18–22). Although soft-tissue tumor detection can benefit greatly by using i.v. contrast agents in human CT, evaluation of soft-tissue tumor models by microCT is severely hampered by the rapid clearance of conventional contrast agents relative to the long imaging times that are required in microCT. The use of targeted contrast agents with a much longer organ or bloodpool half life represents one solution (23). For the case of colorectal tumors, however, protrusion into the bowel lumen provides an intrinsic contrast gradient that makes i.v. contrast unnecessary for detection. The same is true for CT colonography in humans, which is typically performed without i.v. contrast and with a low-dose technique.

The primary goal of our study was to develop a successful method for microCT colonography and evaluate its ability to detect and register colorectal tumors in a mouse model. The combination of recent advances in microCT imaging and mouse modeling of human colorectal cancer made this study possible. Our results indicate that microCT colonography is a sensitive technique for the noninvasive detection of colorectal polyps as small as 2 mm. Detection rates of 80–90% or more were seen for polyps ranging in size from 2 to 5 mm (mean size, 3.0 mm). Detection of tumors <2 mm in diameter could be attributed, in part, to motion artifacts created by peristalsis and respiration. No attempts were made to gate data acquisition to respiration or to minimize peristaltic motion by administration of glucagon. It is likely that detection confidence could be enhanced under motion-suppressed conditions. But it was apparent that most mice contained a polyp at least 2 mm in size and that these would be much easier to follow serially in response to treatment. In addition, luminal fecal pellets were easily distinguished from true soft-tissue lesions. On a per-mouse basis, the accuracy of microCT approaches 100% in evaluating the presence or absence of at least one polyp measuring at least 2 mm. These findings suggest that longitudinal evaluation for monitoring tumor progression or response to various therapies or interventions is now technically feasible by using our microCT colonography method. We anticipate further refinements in our technique, including modifications in the bowel preparation such as a flush with warm PBS, substitution of air or carbon dioxide for corn oil as a negative luminal contrast agent, treatment with glucagon to limit peristalsis, and switching from 2D to 3D assessment.

There are limitations to our study. (The sample size is relatively small and may preclude certain definitive conclusions.) However, we believe that our findings establish proof of concept. Although 3D virtual colonography has proven more accurate than 2D analysis in humans (3), we have not yet completed our attempt to evaluate the accuracy of 3D interpretation. Finally, we recognize that the ionizing radiation associated with microCT scanning dose could potentially effect tumor growth characteristics and thus interfere with serial monitoring of tumor response to anticancer treatments. A recent report analyzed the potential therapeutic effect of microCT in a mouse lung tumor model and found no therapeutic differences between tumor-bearing mice that underwent five sequential medium-resolution microCT scans and a control cohort that was not scanned. This radiation dose is an important concern that is undergoing further investigation (24).

In conclusion, microCT colonography allows for reliable noninvasive detection and registration of polyps as small as 2 mm for the mouse tumor model we have studied. Accurate scanning of live mice with microCT indicates that longitudinal monitoring of tumor growth and response to therapy should now be feasible. The results of future studies with microCT colonography could serve as a direct preclinical bridge to studies involving human subjects.

This paper is dedicated to the memory of Robert Hoeger. We thank William F. Dove for providing financial support to R.B.H. and the freedom to pursue new experimental approaches, a critical assessment of this study, and the sponsorship of this paper. We also thank Linda Clipson for helping with the preparation and submission of this paper. This study was supported by financial assistance from the University of Wisconsin Medical School, Department of Radiology, and Comprehensive Cancer Center; and National Cancer Institute Grants P20 CA86278 (Pre-*In Vivo* Cellular and Molecular Imaging Center grant), R21 CA95249, R37 CA63677 (to William F. Dove), and U01 CA84227 (to William F. Dove).

1. Jemal, A., Tiwari, R. C., Murray, T., Ghafoor, A., Samuels, A., Ward, E., Feuer, E. J. & Thun, M. J. (2004) *Cancer J. Clin.* **54,** 8–29.
2. Bond, J. H. (2003) *Endoscopy* **35,** S35–S40.
3. Pickhardt, P. J., Choi, J. R., Hwang, I., Butler, J. A., Puckett, M. L., Hildebrandt, H. A., Wong, R. K., Nugent, P. A., Mysliwiec, P. A. & Schindler, W. R. (2003) *N. Engl. J. Med.* **349,** 2189–2198.
4. Pickhardt, P. J., Nugent, P. A., Mysliwiec, P. A., Choi, J. R. & Schindler, W. R. (2004) *Ann. Intern. Med.* **141,** 352–359.
5. Pickhardt, P. J. (2003) *Am. J. Roentgenol.* **181,** 1599–1606.
6. Pickhardt, P. J. (2004) *Radiographics* **24,** 1535–1559.
7. Pickhardt, P. J. (2004) *Abdominal Imaging* **29,** 1–4.
8. Paulus, M. J., Gleason, S. S. & Easterly, M. E. (2001) *Lab. Anim.* **30,** 1–10.
9. Paulus, M. J., Gleason, S. S., Kennel, S. J., Hunsicker, P. R. & Johnson, D. K. (2000) *Neoplasia* **2,** 62–70.
10. Moser, A. R., Pitot, H. C. & Dove, W. F. (1990) *Science* **247,** 322–324.
11. Hedlund, L. W., Johnson, G. A. & Mills, G. I. (1986) *Invest. Radiol.* **21,** 843–846.
12. Yang, Y., Tai, Y. C., Siegel, S., Newport, D. F., Bai, B., Li, Q., Leahy, R. M. & Cherry, S. R. (2004) *Phys. Med. Biol.* **49,** 2527–2545.
13. Contag, P. R., Olomu, I. N., Stevenson, D. K. & Contag, C. H. (1998) *Nat. Med.* **4,** 245–247.
14. Kurth, A. A. & Muller, R. (2001) *Skeletal Radiol.* **30,** 94–98.
15. Genant, H. K., Gordon, C., Jiang, Y., Link, T. M., Hans, D., Majumdar, S. & Lang, T. F. (2000) *Hormone Res.* **54,** S24–S30.
16. Issever, A. S., Walsh, A., Lu, Y., Burghardt, A., Lotz, J. C. & Majumdar, S. (2003) *Spine* **28,** 123–128.
17. Laib, A., Kumer, J. L., Majumdar, S. & Lane, N. E. (2001) *Osteoporosis Int.* **12,** 936–941.
18. Cavanaugh, D., Johnson, E., Price, R. E., Kurie, J., Travis, E. L. & Cody, D. D. (2004) *Mol. Imaging* **3,** 55–62.
19. Langheinrich, A. C., Bohle, R. M., Greschus, S., Hackstein, N., Walker, G., von Gerlach, S., Rau, W. S. & Holschermann, H. (2004) *Radiology* **231,** 675–681.
20. Bentley, M. D., Ortiz, M. C., Ritman, E. L. & Romero, J. C. (2002) *Am. J. Physiol.* **282,** R1267–R1279.
21. Garcia-Sanz, A., Rodriguez-Barbero, A., Bentley, M. D., Ritman, E. L. & Romero, J. C. (1998) *Hypertension* **31,** 440–444.
22. Holdsworth, D. W. & Thornton, M. M. (2002) *Trends Biotechnol.* **20,** S34–S39.
23. Weichert, J. P. (2004) in *Mouse Models of Human Cancer*, ed. Holland, E. C. (Wiley, New York), pp. 339–348.
24. Boone, J. M., Velazquez, O. & Cherry, S. R. (2004) *Mol. Imaging* **3,** 149–158.